User's Guide for Hysteretic Capillary Pressure and Relative Permeability Functions in TOUGH2

Christine Doughty
Earth Sciences Division
Lawrence Berkeley National Laboratory

March 2013

1. Background

The precursor of TOUGH2, TOUGH, was originally developed with non-hysteretic characteristic curves. Hysteretic capillary pressure functions were implemented in TOUGH in the late 1980s by Niemi and Bodvarsson (1988), and hysteretic capillary pressure and relative permeability functions were added to iTOUGH2 about ten years later by Finsterle et al. (1998). Recently, modifications were made to the iTOUGH2 hysteretic formulation to make it more robust and efficient (Doughty, 2007). Code development is still underway, and the current hysteresis formulation has now been added to standard TOUGH2 (Pruess et al., 2012).

This document provides a user's guide for the most recent version of the hysteretic code, which runs within iTOUGH2 (Finsterle, 1999a,b,c) or TOUGH2 V2.1 (Pruess et al., 2012). The usage of the hysteretic module is the same in both codes, which for brevity here are both referred to simply as TOUGH2. The current code differs only slightly from what was presented in Doughty (2007), hence that document provides the basic information on the processes being modeled and how they are conceptualized. This document focuses on a description of the user-specified parameters required to run hysteretic TOUGH2. In the few instances where the conceptualization differs from that of Doughty (2007), the features described here are the current ones.

Sample problems presented in this user's guide use the equation-of-state module ECO2N (Pruess, 2005). The components present in ECO2N are H_2O, NaCl, and CO_2. Two fluid phases and one solid phase are considered: an aqueous phase, which primarily consists of liquid H_2O and may contain dissolved NaCl and CO_2; a supercritical phase which primarily consists of CO_2, but also includes a small amount of gaseous H_2O; and a

solid phase consisting of precipitated NaCl. Details of the ECO2N formulation may be found in Pruess (2005). The aqueous phase is the wetting phase and is denoted 'liquid', whereas the supercritical phase is the non-wetting phase and is denoted 'gas'. The hysteretic formalism may be applied to other TOUGH2 equation-of-state modules that consider two fluid phases, as long as the liquid phase is the wetting phase and the gas phase is the non-wetting phase.

2. Characteristic-Curve Functional Forms

The basic equation for capillary pressure P_c as a function of liquid saturation S_l is adapted from the van Genuchten (1980) formulation, and is given by

$$P_c = -P_0^p \left[\left(\frac{S_l - S_{l\min}}{1 - S_{gr}^{\Delta} - S_{l\min}} \right)^{-\left(\frac{1}{m^p}\right)} - 1 \right]^{(1-m^p)}, \tag{1}$$

where p identifies the flow process, drainage (d) or imbibition (w), that is occurring. The parameters P_0^d, P_0^w, m^d, m^w, and $S_{l\min}$ are specified in the ROCKS or RPCAP blocks of the TOUGH2 input file (see below for details). The parameter S_{gr}^{Δ}, the residual gas saturation, depends on the saturation history of the grid block through the turning- point saturation S_l^{Δ}, which identifies the transition from drainage to imbibition for a particular grid block. Following Land (1968), we take

$$S_{gr}^{\Delta} = \frac{1}{1/(1 - S_l^{\Delta}) + 1/S_{gr\max} - 1/(1 - S_{lr})}, \tag{2}$$

where $S_{gr\max}$ and S_{lr} are maximum residual gas saturation and residual liquid saturation, respectively, which are material properties specified in the ROCKS or RPCAP blocks (see below for details). Equation (2) indicates that smaller values of S_l^{Δ} produce larger values of S_{gr}^{Δ}. In other words, the locations that once held the most CO_2 (small S_l^{Δ}), become the locations that trap the most CO_2 (large S_{gr}^{Δ}). Equation (1) provides the so-called primary drainage and primary imbibition capillary pressure curves. During a simulation, the actual capillary pressure curve being followed is determined by interpolation between the two primary curves, as described in Finsterle et al. (1998) and illustrated in Doughty (2007). Interpolated curves are known as scanning curves. In total, four branches of the capillary pressure curve are defined: 1 – primary drainage, 2 – first-order scanning imbibition, 3 – second-order scanning drainage, 4 – third-order scanning imbibition.

The relative permeability functions also include hysteretic effects arising from the trapped component of the gas phase that develops during imbibition. These functions are taken from Parker and Lenhard (1987) and Lenhard and Parker (1987), who adapted them from the non-hysteretic expressions of van Genuchten (1980). As implemented here, the relative permeability to liquid k_{rl} is given by

$$k_{rl} = \sqrt{\bar{S}_l}\left[1 - \left(1 - \frac{\bar{S}_{gt}}{1-\bar{S}_l^{\Delta}}\right)\left(1-(\bar{S}_l+\bar{S}_{gt})^{1/m}\right)^m - \left(\frac{\bar{S}_{gt}}{1-\bar{S}_l^{\Delta}}\right)\left(1-(\bar{S}_l^{\Delta})^{1/m}\right)^m\right]^2 \tag{3}$$

and the relative permeability to gas k_{rg} is given by

$$k_{rg} = k_{rg\max}(1-(\bar{S}_l+\bar{S}_{gt}))^{\gamma}(1-(\bar{S}_l+\bar{S}_{gt})^{1/m})^{2m}, \tag{4}$$

where $\bar{S}_l$ and $\bar{S}_l^{\Delta}$ are effective values of liquid saturation S_l and turning-point saturation S_l^{Δ}, respectively, normalized with respect to residual liquid-phase saturation S_{lr}:

$$\bar{S}_l = \frac{S_l - S_{lr}}{1 - S_{lr}} \tag{5}$$

$$\bar{S}_l^{\Delta} = \frac{S_l^{\Delta} - S_{lr}}{1 - S_{lr}} . \tag{6}$$

The parameter $\bar{S}_{gt}$ is the effective value of the trapped gas-phase saturation:

$$\bar{S}_{gt} = \frac{S_{gr}^{\Delta}(S_l - S_l^{\Delta})}{(1 - S_{lr})(1 - S_l^{\Delta} - S_{gr}^{\Delta})} . \tag{7}$$

The parameters S_{lr}, γ, m, and $k_{rg\max}$ are specified in the ROCKS or RPCAP blocks of the TOUGH2 input file (see below for details). Unlike the capillary pressure algorithm, where Equation (1) merely provides the envelope functions within which interpolation determines the actual capillary pressure curve, Equations (3) and (4) provide the actual relative permeabilities for both drainage and imbibition. The only difference between the two processes is that $\bar{S}_{gt}$ is zero for the primary drainage curve, and non-zero for the scanning curves. Moreover, $\bar{S}_{gt}$ has the same value for all scanning curves, implying that the relative permeability curves have only two branches: one for primary drainage and the other for everything else.

Equation (1) is not defined for $S_l < S_{l\min}$ or $S_l > (1 - S_{gr}^{\Delta})$, Equations (3) and (4) are not defined for $S_l < S_{lr}$, and Equation (3) has an infinite derivative for $S_l = (1 - S_{gr}^{\Delta})$. However, characteristic curves must be defined over the entire liquid saturation domain

from zero to one, because even when a phase is immobile, and hence unable to move by pressure forces, its saturation can change due to other processes (e.g., evaporation of liquid water, dissolution of supercritical CO_2). Hence, the basic hysteretic characteristic curves given by Equations (1), (3), and (4) must be augmented by extensions. Figures 1 and 2 illustrate the key features of the extended hysteretic characteristic curves.

Figure 1 shows the features of the extended hysteretic capillary pressure function. The imbibition branch P_c^w is illustrated for a value of $S_l^\Delta = 0.3$, meaning that for this particular grid block located near a CO_2 injection location, liquid saturation began at $S_l = 1$, decreased until $S_l = 0.3$ as CO_2 entered the grid block, then began to increase again after CO_2 injection ceased. In practice, S_l^Δ can range from S_{lr} to 1.

In Equation (1), P_c goes to infinity at $S_l = S_{l\min}$. In the extended formulation, the P_c defined by Equation (1) is smoothly connected to an exponential or power-law extension that remains finite for all values of S_l. The transition to the extension is controlled by the user-specified variable $P_{c\max}$, which is the value of Equation (1) at S_m, the point where the two functions meet. For the exponential extension, as $P_{c\max}$ increases, S_m decreases (i.e., gets closer to $S_{l\min}$) and the slope of Equation (1) at S_m increases. Thus, the slope of the extension at S_m must also increase, hence its maximum value $P_c(S_l = 0)$ also increases. For the power-law extension, the user specifies the value of $P_c(S_l = 0)$ explicitly. The power-law extension has zero slope at $S_l = 0$.

At the other end of the saturation range, two user options are available for extending the imbibition branch P_c^w for $S_l > S_l^*$, where S_l^* is defined as $1 - S_{gr}^\Delta$. Either P_c^w can go to zero at S_l^*, or P_c^w can gradually decline to zero at $S_l = 1$ following a power-law function.

Figure 2 shows the features of the extended hysteretic relative permeability (k_{rl} and k_{rg}) functions. Previously (Doughty, 2007), when $S_l = S_{lr}$, $k_{rl} = 0$ and $k_{rg} = 1$. The requirement $k_{rg} = 1$ at $S_l = S_{lr}$ has been relaxed, and the user now specifies the value of $k_{rg}(S_{lr})$, which is denoted $k_{rg\max}$. If $k_{rg\max} = 1$, there is no difference from the previous formulation. However, if $k_{rg\max} < 1$, then there are two options for k_{rg} for the saturation range $0 < S_l < S_{lr}$. In either case, k_{rg} increases from $k_{rg\max}$ to 1 as S_l decreases from S_{lr} to 0, but the variation can either be linear or cubic. If the linear option is chosen, a small cubic spline is added at S_{lr}, to guarantee the continuity and smoothness of the extension and original function (this spline is present in Figure 2, but is too small to see). Although S_l^{Δ} can be as small as S_{lr}, meaning that an imbibition curve could originate at S_{lr}, the k_{rg} extension below S_{lr} is only smoothly connected to the drainage branch k_{rg}^{d}. In other words, there is no hysteresis along the extension.

At the other end of the saturation range, Equation (3) cannot be used during imbibition all the way to $S_l = S_l^*$ because the slope k_{rl}^w becomes infinite there, which yields the non-physical consequence of $k_{rl}^w = 1$ at $S_l = S_l^*$. Physically, one must have $k_{rl}^w = 1$ at $S_l = 1$. A convenient means to achieve this is to use the drainage branch k_{rl}^d for both drainage and imbibition when $S_l > S_l^*$. To obtain a smooth connection between k_{rl}^w and k_{rl}^d, a small cubic spline is introduced. The user specifies the width over which the spline extends.

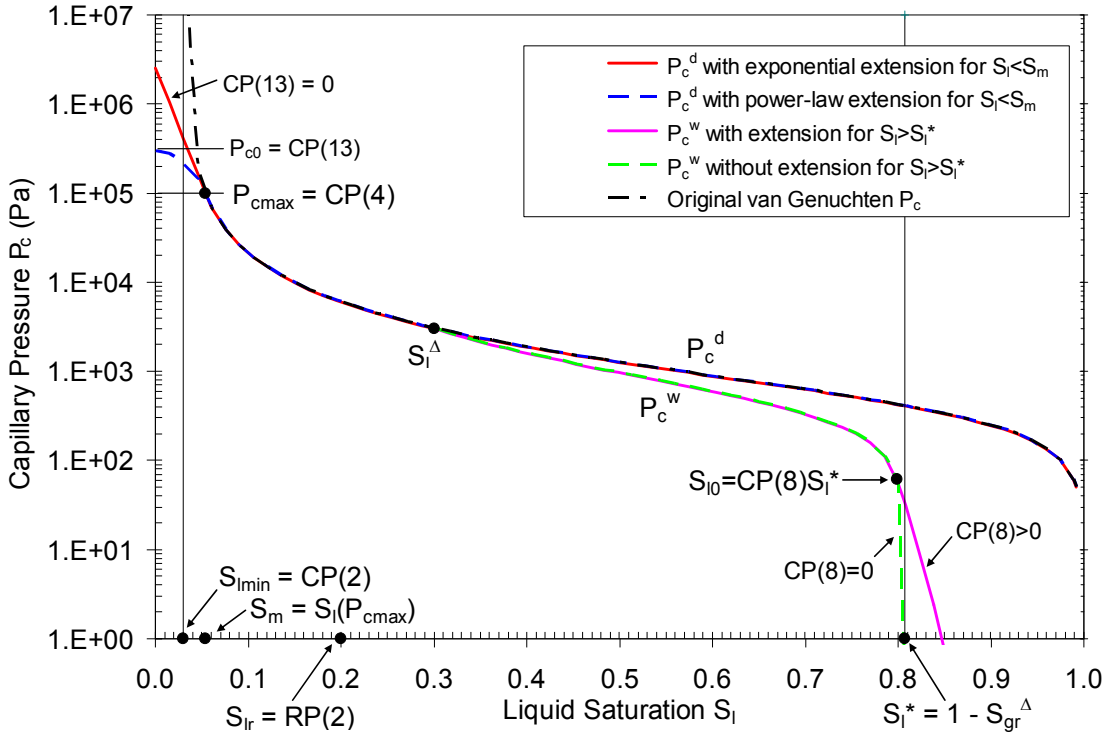

Figure 1. Features of the extended hysteretic capillary pressure function. P_c^w is shown for a typical value of $S_l^\Delta = 0.3$. In practice, S_l^Δ can range from S_{lr} to 1, with S_l^* increasing as S_l^Δ increases.

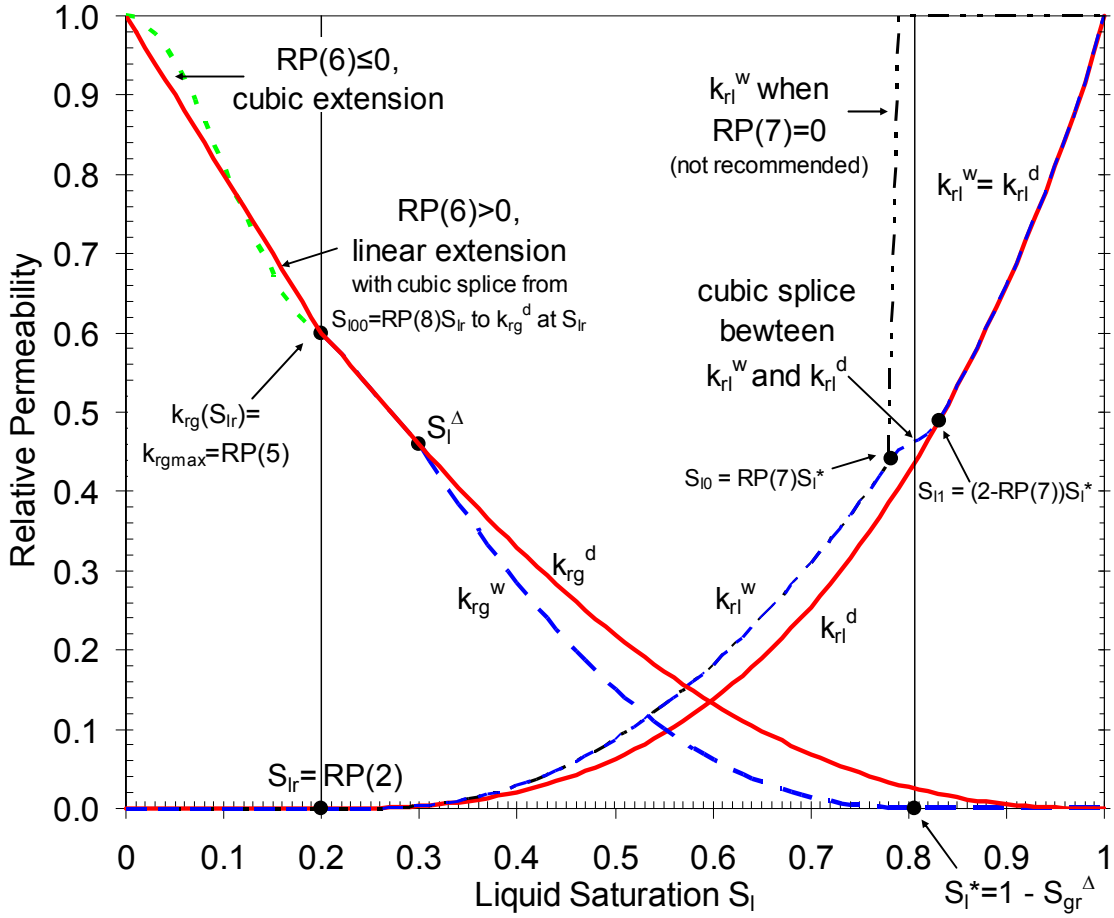

Figure 2. Features of the extended hysteretic relative permeability functions.

3. Input Parameters

3.1 Characteristic Curves

To accommodate the parameters required to specify hysteretic problems, two lines are read in for both relative permeability parameters and capillary pressure parameters. For non-hysteretic materials (IRP≠12, ICP≠12), the second line should not be present. The format for the first line is the usual (I5,5X,7E10.4) and the format for the second line is (8E10.4). Note that the use of this format requires that decimal points be present in all RP and CP entries, even if they are flags that would normally be thought of as integers.

An Excel spreadsheet containing the hysteretic formulations for capillary pressure and relative permeability, newhyster.xls, is distributed along with this user's guide. It is strongly recommended to input the chosen RP and CP parameters into the spreadsheet and examine the resulting capillary pressure and relative permeability curves for a variety of potential turning points prior to running a TOUGH simulation. This exercise will help guide the choice of numerical factors used to produce smooth curves, and may help avoid potential problems that can arise when using extreme values of some variables.

IRP = 12 (must use with ICP = 12)

RP(1) = m; van Genuchten m for liquid relative permeability (need not equal CP(1) or CP(6)); k_{rl} uses same m for drainage and imbibition.

RP(2) = S_{lr}; residual liquid saturation: $k_{rl}(S_{lr}) = 0$, $k_{rg}(S_{lr}) = k_{rg\max}$. Must have $S_{lr} > S_{lmin}$ in capillary pressure (CP(2)). S_{lr} is minimum saturation for transition to imbibition branch. For $S_l < S_{lr}$, curve stays on primary drainage branch even if S_l increases.

RP(3) = $S_{gr\max}$; maximum possible value of residual gas saturation S_{gr}^{Δ}. Note that the present version of the code requires that $S_{lr} + S_{gr\max} < 1$, otherwise there will be saturations for which neither fluid phase is mobile, which the code cannot handle. Setting $S_{gr\max} = 0$ effectively turns off hysteresis. As a special option, a constant, non-zero value of S_{gr} may be employed by setting CP(10)>1 and making RP(3) negative. The code will set S_{gr}^{Δ} = -RP(3) for all grid blocks at all times.

RP(4) = γ; exponent in k_{rg} (default 1/3); typical values 1/3 – 1/2. In Doughty (2007), γ was hardwired at 1/3. For k_{rg}^{d} to replicate the Corey (1954) k_{rg} function, set RP(4) = γ = 2.0, RP(5) = k_{rgmax} = 1.0, and RP(10) = m_{gas} = 0.5 (see Equation (4)).

RP(5) = $k_{rg\max} = k_{rg}(S_{lr})$ (default 1.0); maximum value of k_{rg} obtained using Equation (3). In Doughty (2007), $k_{rg\max}$ was hardwired at 1.0.

RP(6) = fitting parameter for k_{rg} extension for $S_l < S_{lr}$ (only used when $k_{rg\max} < 1$); determines type of function for extension and slope of k_{rg} at S_l= 0.

≤ 0 use cubic spline for $0 < S_l < S_{lr}$, with slope at $S_l = 0$ of RP(6)
> 0 use linear segment for $0 < S_l <$ RP(8)S_{lr} and cubic spline for RP(8)$S_{lr} < S_l < S_{lr}$, with slope at $S_l = 0$ of -RP(6).

RP(7) = numerical factor used for cubic spline connecting k_{rl}^w to k_{rl}^e for $S_l > S_l^*$,. RP(7) is the fraction of S_l^* at which k_{rl}^w curve departs from the original van Lenhard and Parker function (Equation (3)). Recommended range of values: 0.92–0.97. For RP(7)=0, k_{rl}=1 for $S_l > S_l^*$ (not recommended). In general, as smaller values of RP(1) = m are used, RP(7) must get smaller as well. Try various combinations of parameters m, RP(7), and S_l^Δ in the spreadsheet newhyster.xls to make sure that the k_{rl} curve does not have sharp oscillations.

RP(8) = numerical factor used for linear k_{rg} extension to $S_l < S_{lr}$ (only used when $k_{rg\max} >$ 1). RP(8) is the fraction of S_{lr} at which the linear and cubic parts of the extensions are joined.

RP(9) = flag to turn off hysteresis for k_{rl} (no effect on P_c and k_{rg}; to turn off hysteresis entirely, set $S_{g\mathrm{rmax}} = 0$ in RP(3)).
=0 hysteresis is on for k_{rl}
≥ 1.0 hysteresis is off for k_{rl} (force k_{rl} to stay on primary drainage branch (k_{rl}^d) at all times)

RP(10) = m_{gas}; van Genuchten m for gas relative permeability (need not equal CP(1) or CP(6)); k_{rg} uses same m_{gas} for drainage and imbibition. If zero or blank, use RP(1) so that $m_{gas} = m$. For k_{rg}^d to replicate the Corey (1954) k_{rg} function, set RP(4) = γ = 2.0, RP(5) = k_{rgmax} = 1.0, and RP(10) = m_{gas} = 0.5 (see Equation (4)).

ICP = 12 (must use with IRP = 12, uses parameters RP(2) and RP(3))

CP(1) = m^d; van Genuchten m for drainage branch $P_c^d(S_l)$.

CP(2) = $S_{l\min}$; saturation at which original van Genuchten P_c goes to infinity. Must have $S_{l\min} < S_{lr}$, where S_{lr} is the relative permeability parameter RP(2).

CP(3) = P_0^d; capillary strength parameter for drainage branch $P_c^d(S_l)$ (Pa).

CP(4) = $P_{c\max}$; maximum capillary pressure (Pa) obtained using original van Genuchten P_c (Equation 1). Inverting Equation (1) for $P_{c\max}$ determines S_m, the transition point between the original van Genuchten function and an extension that stays finite as S_l goes to zero. For functional form of extension, see description of CP(13) below.

CP(5) = scale factor for pressures for unit conversion (default1.0 for pressure in Pa).

CP(6) = m^w; van Genuchten m for imbibition branch $P_c^w(S_l)$. Default value is CP(1) (recommended unless compelling reason otherwise).

CP(7) = P_0^w; capillary strength parameter for imbibition branch $P_c^w(S_l)$ (Pa). Default value is CP(3) (recommended unless compelling reason otherwise).

CP(8) = parameter indicating whether to invoke non-zero P_c extension for $S_l > S_l^* = 1 - S_{gr}^{\Delta}$

=0 no extension; $P_c = 0$ for $S_l > S_l^*$

>0 power-law extension for $S_l^* < S_l < 1$, with $P_c = 0$ when $S_l = 1$. A non-zero CP(8) is the fraction of S_l^* at which the P_c curve departs from the original van Genuchten function. Recommended range of values: 0.97–0.99.

CP(9) = flag indicating how to treat negative radicand, which can arise for $S_l > S_l^{\Delta 23}$ for second-order scanning drainage curves (ICURV = 3), where $S_l^{\Delta 23}$ is the turning-point saturation between first-order scanning imbibition (ICURV = 2) and second-order scanning drainage. None of the options below have proved to be robust under all circumstances. If difficulties arise because $S_l > S_l^{\Delta 23}$ for ICURV = 3, also consider using IEHYS(3) > 0 or CP(10) < 0, which should minimize the occurrence of $S_l > S_l^{\Delta 23}$ for ICURV = 3.

≤ 0 radicand = max(0,radicand) regardless of S_l value

≤1.0 if $S_l > S_l^{\Delta 23}$, radicand takes value of radicand at $S_l = S_l^{\Delta 23}$

>1.0 if $S_l > S_l^{\Delta 23}$, use first-order scanning imbibition curve (ICURV = 2)

CP(10) = threshold value of $|\Delta S|$ (absolute value of saturation change since previous time step) for enabling a branch switch (default is 1E-6; set to any negative number to do a branch switch no matter how small $|\Delta S|$ is; set to a value greater than 1 to never do a branch switch). See also IEHYS(3). If many oscillations between branches are occurring for small values of $|\Delta S|$, it is tempting to increase CP(10). This has proved successful for some problems, but can cause additional trouble of its own, as it will be easier for grid blocks to remain on the "wrong side" of a turning point. If a larger value of CP(10) is used, it is highly recommended to use IEHYS(3)>0.

CP(11) = threshold value of S_{gr}^{Δ}. If value of S_{gr}^{Δ} calculated from S_l^{Δ} (Equation (2)) is less than CP(11), use $S_{gr}^{\Delta} = 0$. Recommended value 0.01–0.03; default is 0.02. If problems arise for grid blocks that barely become two-phase, then increasing CP(11) may help.

CP(12) = flag to turn off hysteresis for P_c (no effect on k_{rl} and k_{rg}; to turn off hysteresis entirely, set $S_{grmax} = 0$ in RP(3)).

=0 hysteresis is on for P_c

≥1.0 hysteresis is off for P_c (switch branches of P_c as usual, but set $S_{gr} = 0$ in P_c calculation. Make sure other parameters of P_c^d and P_c^w are the same: CP(1) = CP(6) and CP(3) = CP(7))

CP(13) = parameter to determine functional form of P_c extension for $S_l < S_{l\min}$ (i.e., $P_c > P_{c\max}$)

=0 exponential extension

>0 power-law extension with zero slope at $S_l = 0$ and $P_c(0)$=CP(13). Recommended value: 2 to 5 times CP(4)=$P_{c\max}$. Should not be less than or equal to CP(4).

Comparison of Hysteretic and Non-Hysteretic Characteristic Curves

The non-hysteretic characteristic curves most comparable to the hysteretic curves described above are the van Genuchten (1980) curves (IRP = ICP = 7). The drainage branches P_c^d and k_{rl}^d of IRP = ICP = 12 are identical to P_c and k_{rl} of IRP = ICP = 7 (but the manner of defining input parameters differs, so the ROCKS or RPCAP blocks need to be modified). However, the functional form of k_{rg} differs for IRP = 7 and IRP = 12, so in general, even for problems involving only drainage, hysteretic and non-hysteretic cases will not produce identical results. But with a special choice of parameters, the IRP = 12 k_{rg}^d function can be set to match the functional form of the Corey Curve k_{rg}, (IRP = 3 or Corey-Curve option for IRP = 7): use RP(4) = γ = 2.0, RP(5) = k_{rgmax} = 1.0, and RP(10) = m_{gas} = 0.5. Note that for drainage, IRP = 12 assumes that S_{gr} = 0, so with IRP = 7, RP(4) = S_{gr} must be set to a small non-zero values (e.g., 1.e-5). The choice of RP(1) = m can make the drainage branch of the IRP = 12 k_{rl} function approximate other common non-hysteretic k_{rl} functions: for a Corey Curve (IRP = 3), take m = 0.78; for a cubic curve (IRP = 6), take m = 0.9. Recall that distinct values can be used for m for k_{rl} (RP(1)) and m_{gas} for k_{rg} (RP(10)) and that smaller m values require smaller values of the numerical factor RP(7), which controls the connection at S_l*, where the imbibition branch of k_{rl} joins the drainage branch.

There are several ways to effectively turn off hysteresis in a material with IRP = ICP = 12, which may be useful for evaluating the impact of hysteresis for a given problem. One can set $S_{gr\max}$ = RP(3) = 0, CP(1) = CP(6), and CP(3) = CP(7). The code will identify turning points and switch from branches as usual, but all the branches will overlie the primary drainage branch. Alternatively, one can set CP(10), the threshold value of $|\Delta S|$ for switching branches, to a value greater than 1.0. Then each grid block will remain on whatever branch it begins on, and its value of S_{gr}^{Δ} will not change (must have IEHYS(3) = 0, see below). There are also options to turn off hysteresis in capillary pressure only (CP(12) ≥ 1.0), and in liquid relative permeability only (RP(9) ≥ 1.0). These two options may be used together or separately. Finally, a special option exists to enable a constant, non-zero value of S_{gr}^{Δ} to be applied to all grid blocks for all times. This is invoked by setting CP(10) > 1.0, IEHYS(3) = 0, and RP(3) = - S_{gr}^{Δ}.

3.2 HYSTE Block Parameters

The HYSTE block is used to provide some numerical controls on the hysteretic characteristic curves. It is not needed if the default values of all its parameters are to be used. The format is (3I5).

IEHYS(1) = flag to print information about hysteretic characteristic curves
- =0 no additional print out
- ≥1 print a one-line message to the output file every time a capillary-pressure branch switch occurs (recommended)

≥2 print a one-line message to the iTOUGH2 message (.msg) file every time the third-order scanning imbibition curve crosses either the first-order scanning imbibition curve or the second-order scanning drainage curve

IEHYS(2) = flag indicating when to apply capillary-pressure branch switching
- =0 after convergence of time step (recommended)
- >0 after each Newton-Raphson iteration

IEHYS(3) = run parameter for sub-threshold saturation change
- =0 no branch switch unless $|\Delta S| > CP(10)$
- >0 allow branch switch after run of IEHYS(3) consecutive time steps for which all $|\Delta S| < CP(10)$ and all ΔS are the same sign. Recommended value 5-10. This option may be useful if the time step is cut to a small value due to convergence problems, making saturation changes very small.

3.3 MOP Parameter

MOP(13) = Flag to control how INCON block is read
- = 0 or 1 read normal INCON block with two lines per element
- = 2 read hysteretic INCON block with seven lines per element. The additional five lines contain history information for elements with ICP = IRP = 12. For non-hysteretic materials, no history information is required; the additional five lines contain zeros and these entries are not used.

Note that if MOP(13)=0 or 1 or if an element does not appear in the INCON block (or if no INCON block is present), then no history information is available. For elements with ICP = IRP = 12, the only initial conditions that can be specified without history information are for single-phase liquid ($P_c = 0$), or for the primary drainage branch of the capillary pressure curve (two-phase liquid-gas or single-phase gas). Initial conditions on imbibition branches or the scanning drainage branch require that MOP(13)=2 so that all relevant history information will be available. The only practical way to obtain this history information is to use the SAVE file from a prior simulation as the INCON block.

4. Output

4.1 Every Time Step

The message printed out each iteration when MOP(1) > 0 includes the variable KTMP0, the temporary value of the variable ICURV, which identifies which branch of the capillary pressure curve is being followed: 0 – single-phase liquid, 1 – primary drainage, 2 – first-order scanning imbibition, 3 – second-order scanning drainage, 4 – third-order scanning imbibition.

If IEHYS(1) > 0, a one-line message is printed each time an element undergoes a branch switch, including the element name, the ICURV value for the old and new branches, and the turning-point saturation ($S_l^{\Delta 12}$, $S_l^{\Delta 23}$, or $S_l^{\Delta 34}$) . This information can be very useful for analyzing simulations that take small time steps due to slow convergence. When time step is small, many successive small (sub-threshold) saturation changes that are individually too small to trigger a branch switch may occur. This can lead to a saturation on the "wrong side" of the turning-point saturation, which can slow convergence. A typical manifestation of this situation is the maximum residual repeatedly occurring at an element that has ICURV=3. Search backward through the output file to find the most recent branch switch for that element (look for the string "*element-name* old curve") and compare the current S_l to $S_l^{\Delta 23}$. If $S_l > S_l^{\Delta 23}$, it may be worthwhile to stop the code, modify option CP(9), CP(10), or IEHYS(3), and restart the code using the SAVE file as the new INCON file.

4.2 Main Output

Columns have been added to show ICURV, the branch of the capillary pressure curve being followed, and SOR, the history-dependent value of residual gas saturation S_{gr}^{Δ}.

4.3 SAVE File

The SAVE file must contain all the information required to do a restart, thus whenever there is at least one hysteretic material (IRP = ICP = 12) in a problem, the save file contains five lines for each element with information on capillary-pressure branch, turning points, etc., in addition to the usual two lines containing element name, porosity, and state variables. For non-hysteretic materials (IRP, ICP $\neq$ 12), the entries in the additional five lines are all zero and are not used. These unused lines are included so that the SAVE file may be used as an INCON file for a subsequent restart.

4.4 Additional Files

File.hys (unit 82) If an element ELST is specified in the PARAM block, and that element has IRP = ICP = 12, then this file contains the values of time, S_l, P_c, ICURV, k_{rg}, and k_{rl} for that element every time step. The file is formatted for Tecplot, but the user needs to edit the file to add the number of entries (after "i=" on line 3), and optionally add title information within the pairs of quotes on lines 1 and 3.

iTOUGH2file.msg If IEHYS(1) $\geq$ 2, a message is printed every time the third-order scanning imbibition curve (ICURV = 4) crosses either the first-order scanning

imbibition curve (ICURV = 2) or the second-order scanning drainage curve (ICURV = 3). Warning: this file can get very big, and probably is only useful for debugging purposes.

5. Sample Problems

5.1 Problem 1: CO_2 Injection with Dry Out and Subsequent Dissolution

A simple one-dimensional problem showing CO_2 injection into a tilted saline aquifer is presented to demonstrate the hysteretic version of TOUGH2 with the ECO2N (identified as EOS17 in iTOUGH2) module, in particular to test the extensions beyond which brine and CO_2 are immobile. Two cases consider different rates and durations of CO_2 injection. In the first case, a relatively small amount of CO_2 is injected to illustrate a range of S_{gr}^{Δ} values. In the second case, CO_2 injection is large enough for elements near the injection location to dry out. In both cases, the simulations continue after CO_2 injection ceases. Hysteretic (IRP = ICP = 12) and non-hysteretic (IRP = ICP = 7) cases are shown to enable comparison. Table 1 summarizes numerical performance of the cases run. See the input files for detailed specification of material properties, including characteristic curves. Parameters are believed reasonable for high-permeability saline formations, and are similar to parameters used to model the Frio brine pilot (Doughty et al., 2008).

Table 1. Job name and CPU time required for 100-year simulations of Problem 1, using a Dell Latitude D800 with 2 GHz clock speed and 2GB RAM.

Amount of CO_2 injected	Hysteretic	Non-hysteretic
1 kg/s CO_2 for 1 day	j203t – 356 steps, 18sec	d2o3t – 304 steps, 13 sec
5 kg/s CO_2 for 5 days	h2o3t – 398 steps, 21 sec	c2o3t – 392 steps, 17 sec

The model is one-dimensional and consists of 100 elements, each 2 m long, tilted at an angle of 10° from the horizontal. CO_2 is injected at a constant rate near the middle of the model. Prior to CO_2 injection, a gravity-equilibration simulation is done for a brine with P = 200 bars, T = 75°C, and a salt content of X_{NaCl} = 0.1. Then, the lowermost and uppermost elements are made inactive to hold pressure fixed at the resulting values. Next, the amount of salt in every element is decreased to X_{NaCl} = 0.03, which results in lower density and a moderate steady upward brine flow through the model. These are the initial conditions for the CO_2 injection. The upward brine flow was chosen to illustrate the dissolution of immobile CO_2.

Results

Figures 3 and 4 show the hysteretic characteristic curves for the injection element for cases j203t and h203t. Figures 5 and 6 show profiles of gas saturation for a series of times, comparing hysteretic and non-hysteretic cases. In all cases, by the end of the 100-year simulation period, all CO_2 has been purged from the system. For the non-hysteretic cases, which have S_{gr} = 0, much of the CO_2 flows out of the model as a free phase. For the hysteretic cases, which have $S_{gr\max}$ = 0.2, a significant fraction of the injected CO_2 becomes immobilized, but it gradually dissolves in the upward-flowing brine that is moving past the trapped CO_2 plume, and eventually flows out of the model in dissolved form.

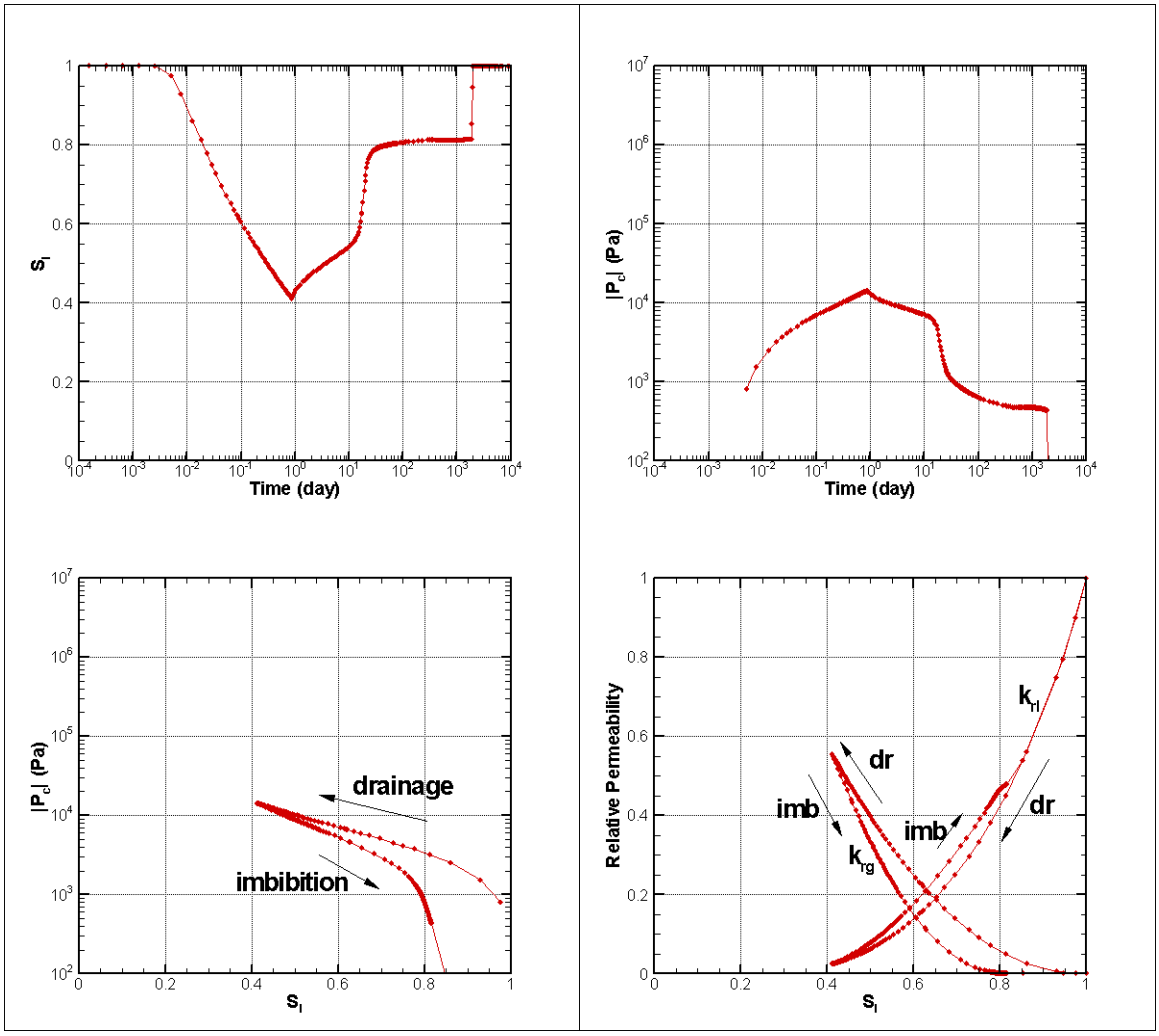

Figure 3. Characteristic curve branches followed for the injection element for Case j203t, in which a small amount of CO_2 is injected for 1 day, followed by 100 years of redistribution.

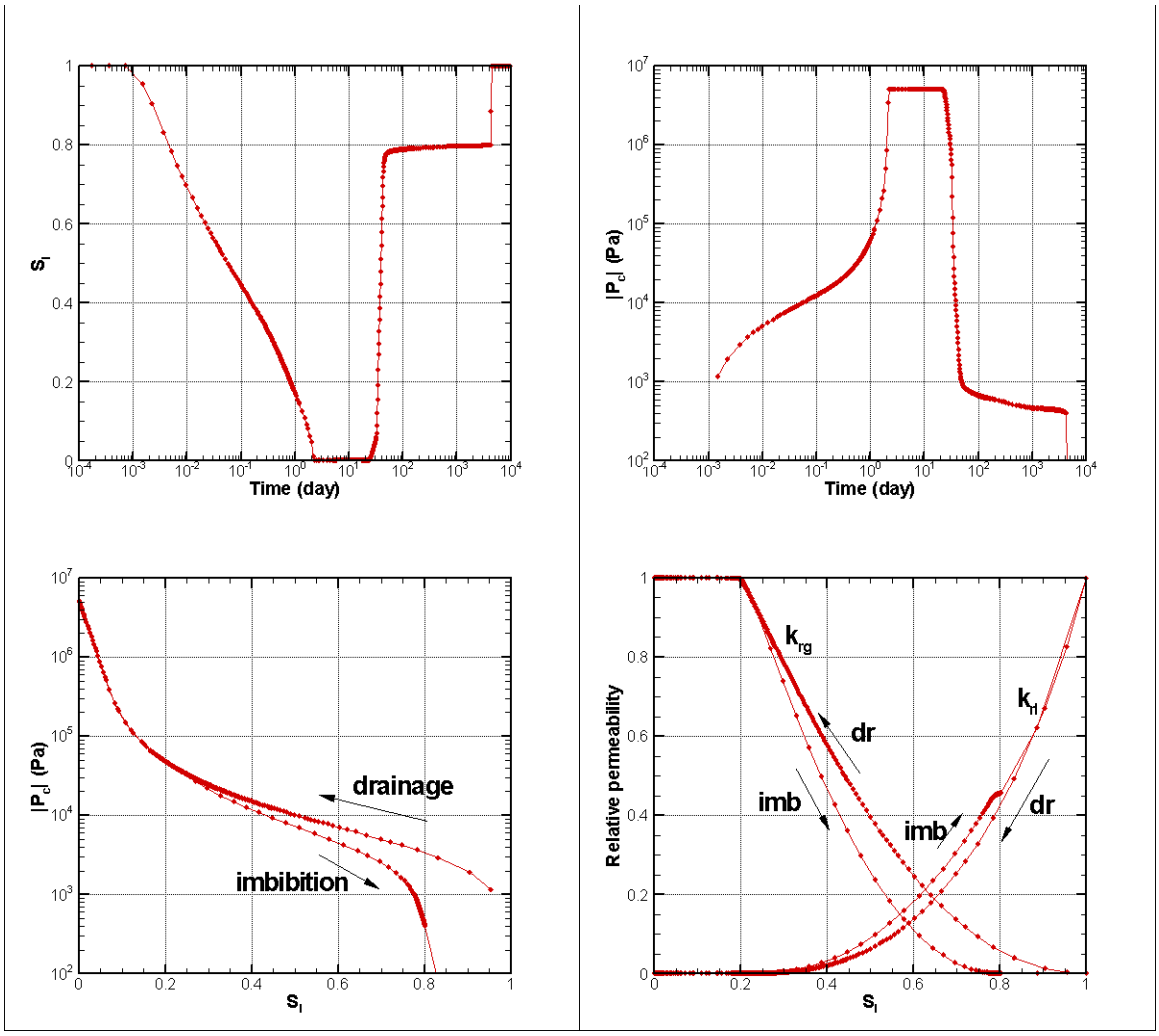

Figure 4. Characteristic curve branches followed for the injection element for Case h203t, in which a large amount of CO_2 is injected for 5 days, followed by 100 years of redistribution.

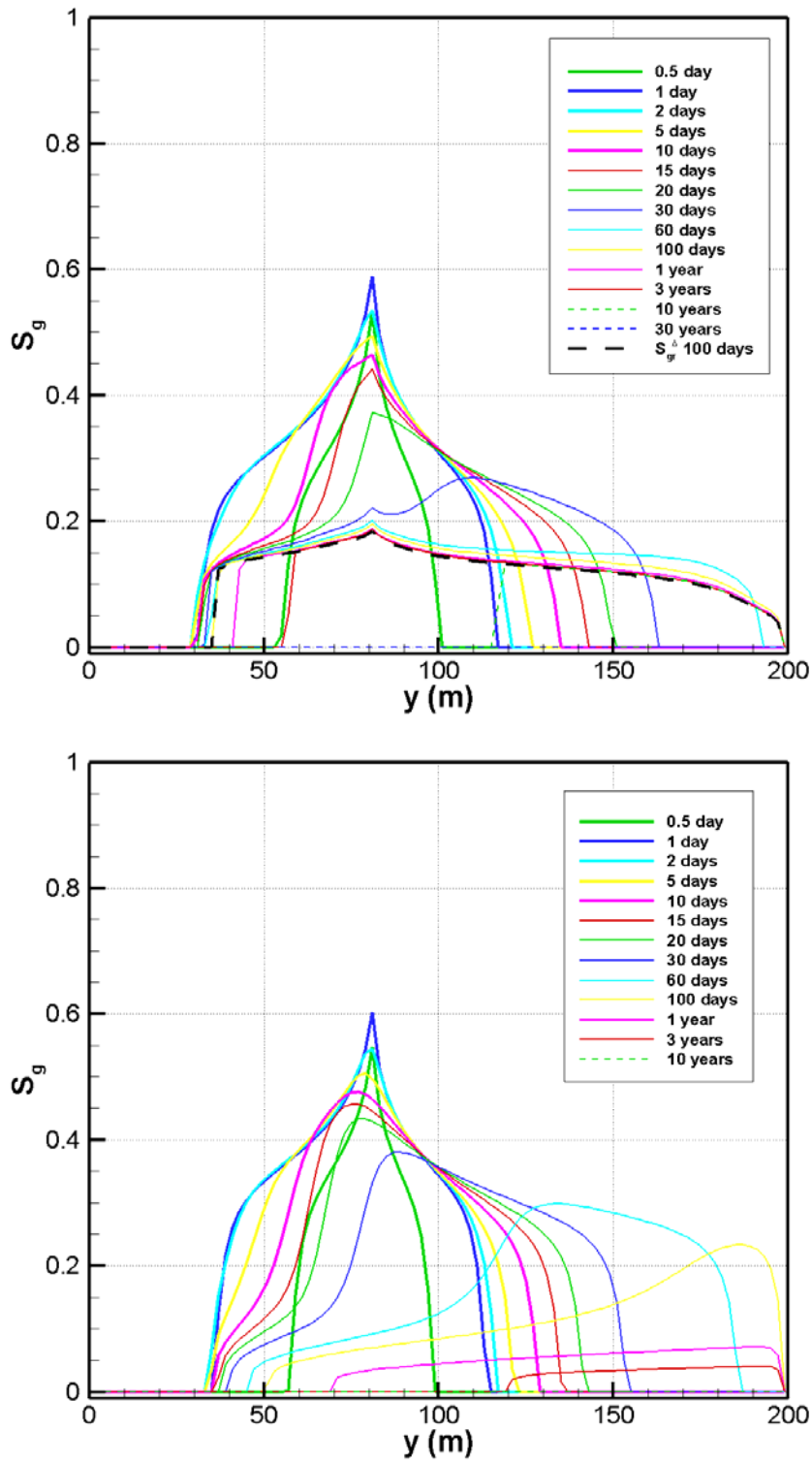

Figure 5. Profiles of S_g versus distance along the model for various times for cases with a small amount of CO_2 injected for 1 day: j203t (with hysteresis, top) and d203t (no hysteresis, bottom). The injection element is located at $y = 81$ m. For the hysteretic case, S_{gr}^{Δ} at 100 days is also shown.

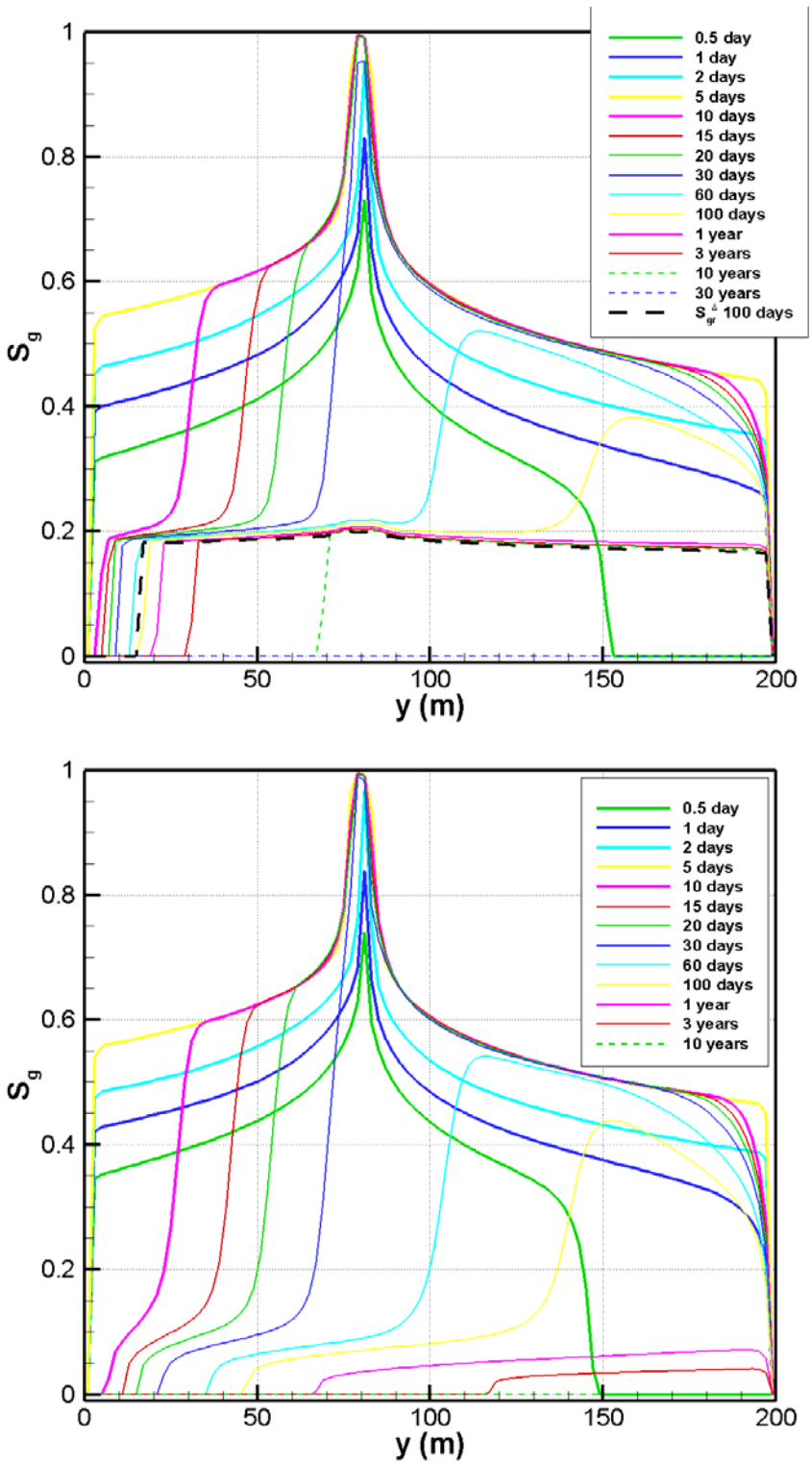

Figure 6. Profiles of S_g versus distance along the model for various times for cases with a large amount of CO_2 injected for 5 days: h203t (with hysteresis, top) and c203t (no hysteresis, bottom). The injection element is located at y = 81 m. For the hysteretic case, S_{gr}^{Δ} at 100 days is also shown.

5.2 Problem 2: Sequence of Repeated CO_2 and H_2O Injection Periods

Problem 2 (developed by Michele Carpita and Alfredo Battistelli of Snamprogetti, Italy) considers a series of successive CO_2 and water injections inside a 240 m long, one-dimensional, horizontal grid without salt and under isothermal conditions. The whole simulation lasts just 60 days, and there is no resting time between any two subsequent injections. The whole grid is initialized at P = 100 bar and T = 50 °C conditions. A boundary element with a fixed pressure of P =100 bar is located at x = 0 in order to induce all the injected fluids to move toward it.

The injection sequence was created in order to test all the branches of the hysteretic curves and the branch-switching processes, without the additional complications of Problem 1 (e.g., gravity flow of both brine and CO_2, CO_2 solubility dependence on salt content). Each injection element is located upgradient with respect to the previous injection element, to avoid spurious effects in the elements far from the fixed boundary.

The injection sequence consists of five steps, detailed as follows, and illustrated in Figure 7:

1) - A first CO_2 injection (2 kg/s for 2 days) in element A1146 (x = 178 m) in order to place the nearby elements along the primary drainage curve (ICURV = 1).

2) – A first H_2O injection (0.01 kg/s for 23 days) in element A1149 (x = 190 m) to put some elements on the first-order imbibition curve (ICURV = 2).

3) - Another CO_2 injection (0.5 kg/s for 5 days) in element A1152 (x = 202 m) to activate the second-order drainage curve (ICURV = 3).

4) - A second H_2O injection (0.5 kg/s for 20 days) in element A1155 (x = 214 m) to activate the third-order imbibition curve (ICURV = 4). The H_2O injection is prolonged so as to let the water saturation increase above the domain of the second-order drainage curve (i.e., to $S_l > S_l^{\Delta 23}$), to check if there is a correct branch switch to the first-order imbibition curve (ICURV = 2).

5) - A final CO_2 injection (1 kg/s for 10 days) in element A1158 (x = 226 m) to see what happens after the third-order imbibition.

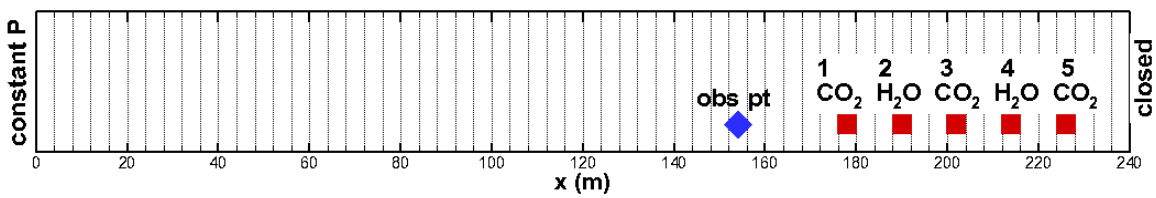

Figure 7. Illustration of the grid, boundary conditions, and source and observation locations for Problem 2.

Results

Figure 8 shows a series of snapshots of the saturation distribution in the model. The overall flow of fluid toward the constant-pressure boundary at x = 0 is evident. Element A1140, which is located at x = 154 m, just downstream of all the injection elements, is chosen as the primary location at which to examine the saturation and capillary pressure variation more closely, as shown in Figure 9.

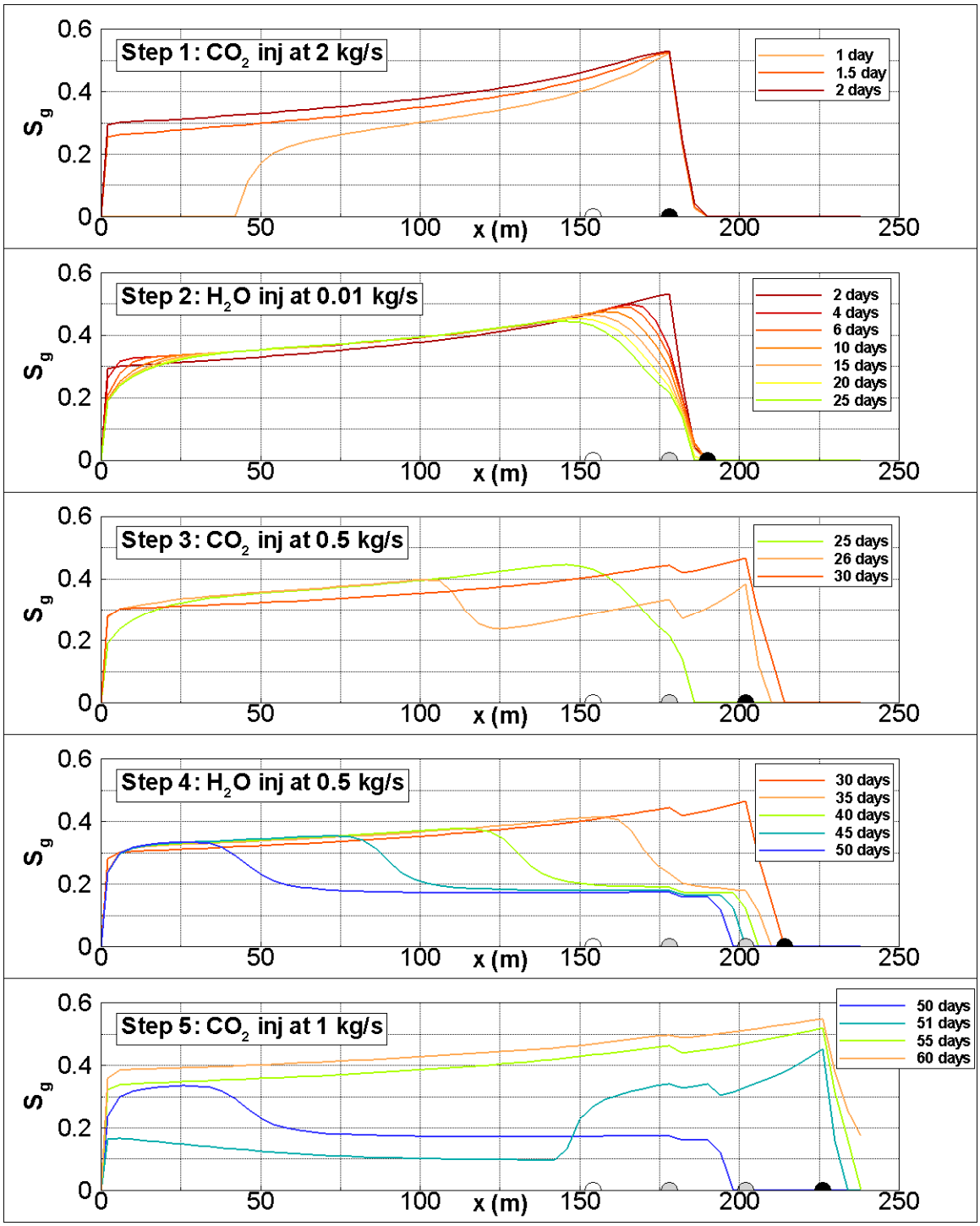

Figure 8. Saturation distributions in the model at various times during the five-step injection sequence. Each injection location is identified with a filled black or grey dot. The location of element A1140 is shown as an open dot.

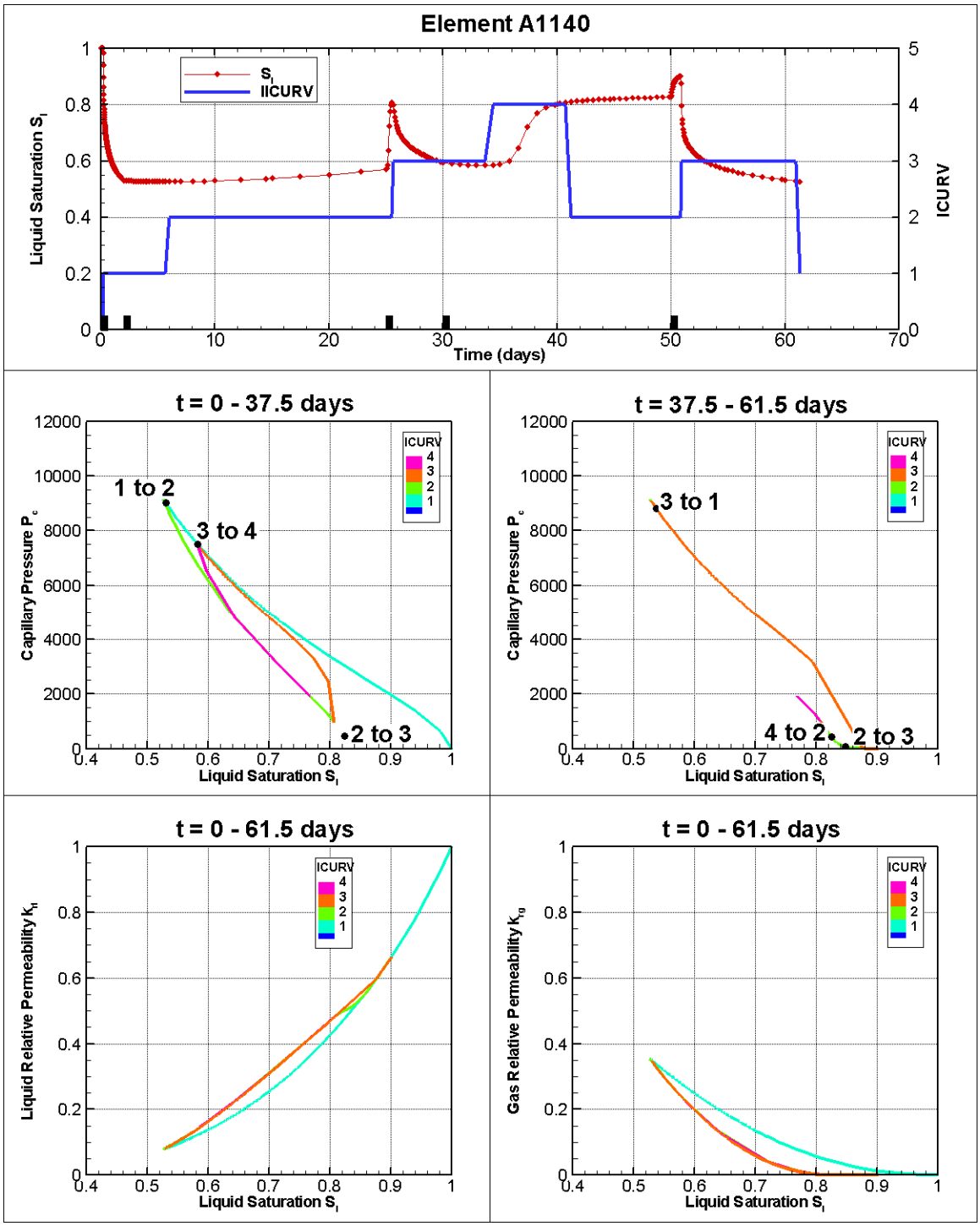

Figure 9. Top: time-variation of liquid saturation and capillary-pressure-curve branch (ICURV) for element A1140. The start of each injection step is marked by a black bar. Middle: capillary pressure versus liquid saturation at element A1140. The plot is divided into two parts, based on time, to enable the different branches of the capillary pressure curve to be seen more easily. The branch switches are marked by black dots, with ICURV for each switch labelled. Bottom: relative permeability versus liquid saturation at element A1140. Branches 2, 3, and 4 all overlie one another.

6. Acknowledgments

Review of this document by Stefan Finsterle of Berkeley Lab is gratefully appreciated. Special thanks go to Michele Carpita and Alfredo Battistelli of Snamprogetti, who carefully examined the code and provided much valuable input for its improvement. This work was supported by the ZERT (Zero Emissions Research and Technology) and GEO-SEQ programs, through the Assistant Secretary for Fossil Energy, Office of Coal and Power Systems through the National Energy Technology Laboratory, and by Lawrence Berkeley National Laboratory under Department of Energy Contract No. DE-AC02-05CH11231.

7. References

Doughty C. Modeling geologic storage of carbon dioxide: comparison of non-hysteretic and hysteretic characteristic curves. Energy Conversion and Management 48(6), 1768-1781, 2007.

Doughty C, Freifeld BM, Trautz RC. Site characterization for CO_2 geologic storage and vice versa: The Frio brine pilot, Texas, USA as a case study. Environmental Geology 54(8), 1635-1656, DOI:10.1007/S00254-007-0942-0, 2008.

Finsterle S. iTOUGH2 user's guide. Rep. LBNL-40040, Lawrence Berkeley National Laboratory, Berkeley, CA, 1999a.

Finsterle S. iTOUGH2 sample problems. Rep. LBNL-40041, Lawrence Berkeley National Laboratory, Berkeley, CA, 1999b.

Finsterle S. iTOUGH2 command reference. Rep. LBNL-40041, Lawrence Berkeley National Laboratory, Berkeley, CA, 1999c.

Finsterle S, Sonnenborg TO, Faybishenko B. Inverse modeling of a multistep outflow experiment for determining hysteretic hydraulic properties. In Pruess K, editor. Proceedings of the TOUGH workshop '98, Rep. LBNL-41995, Lawrence Berkeley National Laboratory, Berkeley, CA, 1998, p. 250-256.

Land CS, Calculation of imbibition relative permeability for two- and three-phase flow from rock properties (SPE 1942), SPE Journal 8(2), 149-156, 1968.

Lenhard RJ, Parker JC. A model for hysteretic constitutive relations governing multiphase flow, 2. Permeability-saturation relations. Water Resources Research 23(12), 2197-205, 1987

Niemi A, Bodvarsson GS. Preliminary capillary hysteresis simulations in fractured rocks, Yucca Mountain, Nevada. Journal of Contaminant Hydrology 3, 277-91, 1988.

Parker JC, Lenhard RJ. A model for hysteretic constitutive relations governing multiphase flow, 1. Saturation-pressure relations. Water Resources Research 23(12), 2187-96, 1987.

Pruess K. ECO2N: A TOUGH2 Fluid Property Module for Mixtures of Water, NaCl, and CO_2. Rep. LBNL-57952, Lawrence Berkeley National Laboratory, Berkeley, CA, 2005.

Pruess K, Oldenburg C, Moridis G, TOUGH2 User's Guide, Version 2.1, Rep. LBNL-43134rev, Lawrence Berkeley National Laboratory, Berkeley, CA, 2012.

van Genuchten MTh. A closed-form equation for predicting the hydraulic conductivity of unsaturated soils. Soil Science Society of America Journal 44(5), 892-898, 1980.

DISCLAIMER

This document was prepared as an account of work sponsored by the United States Government. While this document is believed to contain correct information, neither the United States Government nor any agency thereof, nor The Regents of the University of California, nor any of their employees, makes any warranty, express or implied, or assumes any legal responsibility for the accuracy, completeness, or usefulness of any information, apparatus, product, or process disclosed, or represents that its use would not infringe privately owned rights. Reference herein to any specific commercial product, process, or service by its trade name, trademark, manufacturer, or otherwise, does not necessarily constitute or imply its endorsement, recommendation, or favoring by the United States Government or any agency thereof, or The Regents of the University of California. The views and opinions of authors expressed herein do not necessarily state or reflect those of the United States Government or any agency thereof or The Regents of the University of California.

Ernest Orlando Lawrence Berkeley National Laboratory is an equal opportunity employer.